Porous Capsules

Deutsche Ausgabe: DOI: 10.1002/ange.201511341
Internationale Ausgabe: DOI: 10.1002/anie.201511341

The Uptake and Assembly of Alkanes within a Porous Nanocapsule in Water: New Information about Hydrophobic Confinement

*Sivil Kopilevich, Hugo Gottlieb, Keren Keinan-Adamsky, Achim Müller, and Ira A. Weinstock**

Abstract: *In Nature, enzymes provide hydrophobic cavities and channels for sequestering small alkanes or long-chain alkyl groups from water. Similarly, the porous metal oxide capsule* $[\{Mo^{VI}{}_6O_{21}(H_2O)_6\}_{12}\{(Mo^{V}{}_2O_4)_{30}(L)_{29}(H_2O)_2\}]^{41-}$ *(L = propionate ligand) features distinct domains for sequestering differently sized alkanes (as in Nature) as well as internal dimensions suitable for multi-alkane clustering. The ethyl tails of the 29 endohedrally coordinated ligands, L, form a spherical, hydrophobic "shell", while their methyl end groups generate a hydrophobic cavity with a diameter of 11 Å at the center of the capsule. As such,* C_7 *to* C_3 *straight-chain alkanes are tightly intercalated between the ethyl tails, giving assemblies containing 90 to 110 methyl and methylene units, whereas two or three ethane molecules reside in the central cavity of the capsule, where they are free to rotate rapidly, a phenomenon never before observed for the uptake of alkanes from water by molecular cages or containers.*

In Nature, unique environments and structures provide for the sequestration, transport, and reactions of small alkanes in water. These range from the formation of methane clathrates (hydrated methane aggregates are referred to as "fire ice") at the bottom of the world's oceans and in the outer regions of our solar system[1] to the uptake of small alkanes by hydrophobic cavities in monooxygenase enzymes.[2] In other enzymes, helical channels of hydrophobic peptides bind long-chain alkyl groups of fatty acids and phospholipids.[3] For synthetic systems in organic solvents, a variety of alkanes,[4] their halogenated derivatives,[5] and other small molecules[5f] have been encapsulated within self-assembled cages, in conjunction with recognition,[6] unprecedented structures,[7] and new reaction pathways.[4] In water, where alkane uptake is controlled by hydrophobic effects, modestly sized hydrocarbons, such as *n*-butane, serve as templates for the assembly of water-soluble cavitands,[8] and longer-chain alkanes exhibit unique packing motifs.[9] Smaller alkane templates, however, such as methane and ethane, are much less effective.[10] By contrast, water-soluble molecular baskets[11] and containers, such as the cyclophanes[12] and cucurbiturils,[5e] all with preformed hydrophobic cavities, effectively sequester methane[13] and stabilize specific conformations of long-chain alkanes.[9,14] At the same time, the interiors of these important containers are too small to simultaneously provide entirely different types of hydrophobic regions or for hosting alkanes in sufficiently larger numbers to investigate their clustering in nanoconfined hydrophobic domains.[15]

We now demonstrate these phenomena for the first time using a water-soluble porous capsule whose interior contains two distinctly different types of hydrophobic domains. The capsule is a derivative of porous $\{Mo_{132}\}$-type nanocapsules with the general formula $[\{Mo^{VI}{}_6O_{21}(H_2O)_6\}_{12}\{Mo^{V}{}_2O_4(L)\}_{30}]^{42-}$ (L = carboxylate ligand), whose unique properties and tunable internal environments render this class of molecular containers particularly suitable for discovering new phenomena,[16] including the influence of nanoconfinement on hydrophobic self-assembly in water.[17]

The capsule used in the present work has the formula $[\{Mo^{VI}{}_6O_{21}(H_2O)_6\}_{12}\{(Mo^{V}{}_2O_4)_{30}(\text{propionate})_{29}(H_2O)_2\}]^{41-}$ (Figure 1).[17d] The ethyl group tails of the 29 endohedrally coordinated propionate ligands form an approximately spherical hydrophobic "shell", while their methyl end groups generate a hydrophobic cavity with a diameter of

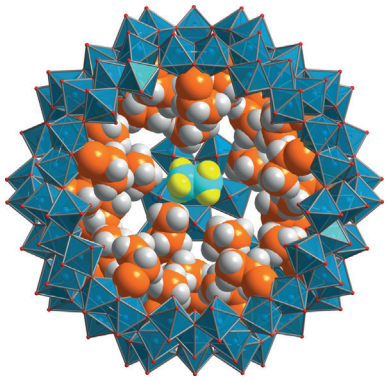

Figure 1. Cut-away view of an ethane molecule in the approximately 700 Å^3 large hydrophobic central cavity of a $\{Mo_{132}\}$-type capsule with 29 endohedrally coordinated propionate ligands. The C and H atoms of ethane are shown in teal and yellow, the C and H atoms of the propionate ligands in orange and white, MoO_6 polyhedra in blue, and the O atoms at their vertices in red. (The drawing of the capsule and its ligands is based on structural data reported in Ref. [17d].)

[*] Dr. S. Kopilevich, Prof. I. A. Weinstock
Department of Chemistry
Ben-Gurion University of the Negev and the Ilse Katz Institute for Nanoscale Science & Technology
Beer Sheva, 84105 (Israel)
E-mail: iraw@bgu.ac.il
Homepage: http://www.bgu.ac.il/~iraw
Dr. H. Gottlieb, Dr. K. Keinan-Adamsky
Department of Chemistry, Bar-Ilan University
Ramat Gan, 529002 (Israel)
Prof. Dr. A. Müller
Fakultät für Chemie, Universität Bielefeld
Postfach 100131, 33501 Bielefeld (Germany)
Supporting information and the ORCID identification number(s) for the author(s) of this article can be found under http://dx.doi.org/10.1002/anie.201511341.

11 Å (ca. 700 Å^3) at the center of the capsule. Reactions with incrementally smaller alkanes (from *n*-heptane to methane) reveal two distinct sites for self-assembly inside the capsule. Whereas larger alkanes (C_7 to C_3, with *n*-butane studied in detail) are tightly intercalated between the propionate ligands, ethane molecules (Figure 1) rotate rapidly in the hydrophobic cavity at the center of the capsule.

Alkane uptake was initially studied by placing liquid *n*-pentane in direct contact with D_2O solutions of an acetate ligand form of the capsule, $[\{Mo^{VI}_6O_{21}(H_2O)_6\}_{12}\{Mo^{V}_2O_4(MeCO_2)_{22}(H_2O)_{16}\}]^{34-}$,[16c] whose porous metal oxide skeleton is shown in Figure 2a. After stirring overnight,

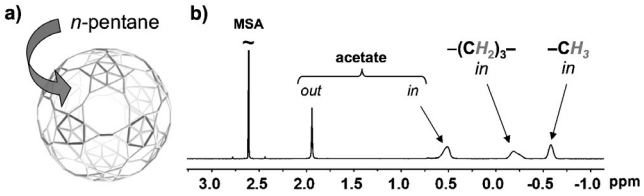

Figure 2. Encapsulation of *n*-pentane by an acetate ligand form of the $\{Mo_{132}\}$-type capsule. a) Ball-and-stick model of the metal oxide skeleton of the capsule. b) ^{1}H NMR spectrum of the D_2O solution after uptake of 6 equiv of *n*-pentane. The broad signal at about 0.5 ppm is due to internally bound acetate anions, while those at approximately −0.2 and −0.6 ppm arise from encapsulated *n*-pentane. The sharp signals at ca. 1.9 and 2.6 ppm are due to acetate anions (1–2 equiv) in the pH 4.5 solution outside the capsule and to an external integration standard (methanesulfonic acid, MSA), respectively.

the *n*-pentane layer was removed, and the D_2O solution was analyzed by ^{1}H NMR spectroscopy (Figure 2b; see the Supporting Information for details).

The ^{1}H NMR signals of the methylene ($-CH_2-$) and methyl ($-CH_3$) protons of encapsulated *n*-pentane appear upfield of those arising from the methyl protons of the internally bound acetate ligands (at ca. 0.5 ppm). As is typical for organic guests encapsulated in $\{Mo_{132}\}$-type complexes, the signals are broad,[16–17] largely owing to restricted motion inside the capsule.

Next, a series of $\{Mo_{132}\}$-type capsules with different carboxylate ligands, RCO_2^- (R = H, Me, Et, *i*Pr, *n*Pr), were exposed to *n*-pentane (liquid layer) for 16 hours at 296 K. The propionate ligand form of the capsule (R = Et) sequestered the largest number of equivalents of *n*-pentane (ca. 8 equiv; see the Supporting Information, Figure S1). Accordingly, the propionate capsule (Figure 3a) was selected for a more detailed investigation of the uptake of a series of alkanes, from *n*-heptane to methane (C_7 to C_1).

In every experiment, the concentration of the $\{Mo_{132}\}$ capsule was 3.61 mM, and the reactions, which were carried out in the presence of excess alkane, were continued until uptake was complete as indicated by no further changes in the ^{1}H NMR spectra of the solutions. The numbers of equivalents of encapsulated alkanes were then determined by quantitative comparison of the ^{1}H NMR signal intensities of the methyl or methylene protons of the sequestered guests with that of an external (co-axial) methanesulfonate (MSA)

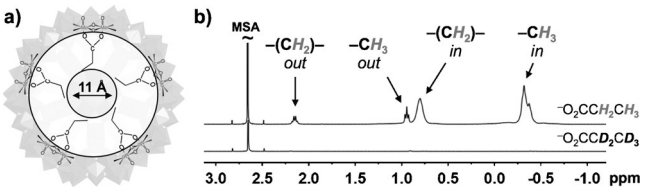

Figure 3. The propionate ligand form of the capsule. a) Two-dimensional cut-away diagram showing endohedrally coordinated propionate ligands and the 11 Å large central cavity formed by their methyl end groups. b) ^{1}H NMR spectra of capsules with propionate ligands (top) and ^{1}H-NMR-silent perdeuterated $[D_5]$-propionate ligands (bottom). The signals labeled "out" in the top spectrum are due to excess propionate ligands in the bulk solution outside the capsule.

integration standard, previously calibrated against solutions of sodium tetraphenylborate (see the Supporting Information for details). However, it soon became apparent that highly precise quantitation was impeded by the overlap of the ^{1}H NMR signals arising from the encapsulated alkanes and the $-CH_2CH_3$ groups of the internally bound propionate ligands (Figure 3b, top spectrum). This problem was circumvented by preparing capsules with perdeuterated $[D_5]$-propionate ligands (Figure 3b, bottom spectrum).

D_2O solutions of the capsules (all at 3.61 mM) with $[D_5]$-propionate ligands were then contacted with liquid phases of the C_7, C_6, and C_5 *n*-alkanes for 16 hours at 296 K. For the reaction with *n*-butane, approximately 100 μL of this hydrocarbon were condensed (at 3 atm and −1 °C) into a gas-tight high-pressure NMR tube containing a D_2O solution of the capsule. The system was then sealed and kept at 296 K for 16 hours, after which the *n*-butane layer was removed by reducing the internal pressure to 1 atm of *n*-butane (and ca. 0.02 atm of D_2O vapor). For propane, ethane, and methane, D_2O solutions of the capsules in gas-tight NMR tubes were exposed to 3 atm of the gaseous hydrocarbons for 16 hours at 296 K, and ^{1}H NMR spectra were obtained directly, that is under 3 atm pressure of each gas. The resultant spectra are shown in Figure 4.

For the C_7, C_6, and C_5 *n*-alkanes, the numbers of equivalents of encapsulated guests were determined by using a co-axial MSA integration standard as described above (its signal, at 2.6 ppm, is shown in Figure 3b). For reactions carried out under pressure, the co-axial tube could not be used. In those cases, formate buffer (its signal at 8.3 ppm is not shown in Figure 4) was used as an internal integration standard (see Figures S2 and S3 for details).

As the hydrocarbon size decreased from C_7 to C_3, the average number of encapsulated alkanes generally increased: 4.4, 6.1, 7.6, 12.7, and 12.5 equivalents after reaction with liquid *n*-heptane, *n*-hexane, *n*-pentane, *n*-butane, and 3 atm of propane, respectively (Figure 4A–E). A dramatic decrease in the number of encapsulated guests was observed for the C_2 and C_1 alkanes (both at 3 atm), with 2.7 and 0.5 equivalents of ethane and methane, respectively, found inside the capsule (F and G). This decrease occurred despite the larger solubilities of these gases in water (2 and 1.4 mM for 1 atm of ethane and methane, respectively, at 293 K; the signals labeled "out" are due to C_2 and C_1 molecules dissolved in D_2O outside the

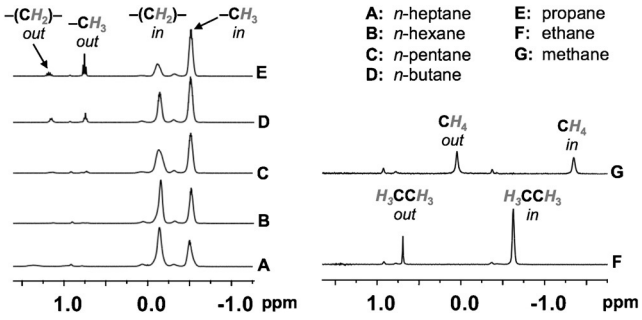

Figure 4. ^{1}H NMR spectra after the encapsulation of C_7 to C_1 alkanes by the [D_5]-propionate form of the {Mo_{132}}-type capsule (3.61 mM in D_2O; each capsule with 29 [D_5]-propionate ligands). In each case, the D_2O solutions were exposed to the liquid or gaseous hydrocarbons for 16 h at 296 K. As the hydrocarbon chain length decreases from C_7 to C_3 (A–E), the intensities of the methyl proton (CH_3) signals at −0.5 ppm increase relative to those of the methylene proton (CH_2) signals at about −0.1 ppm, in line with the increasing CH_3/CH_2 ratio. The *n*-butane observed in bulk solution outside the capsule in plot D is mainly due to numerous small bubbles of the gas, whereas for propane, ethane, and methane (E–G), the signals in bulk solution are due to the dissolved alkanes.

capsule). Confirmation that the upfield signals were indeed due to encapsulation was obtained by diffusion ordered NMR spectroscopy (DOSY)[18a] (Figure S4).

An informative parameter for comparing the occupancy of the capsule by the different alkane guests is the average number of encapsulated carbon atoms (i.e., the sum of the methyl and methylene carbon atoms; Figure 5). This number was consistently large for the C_7 to C_3 alkanes, with sums of 31, 37, 38, 51, and 38, respectively, representing 4–5, 6–7, 7–8, 12–13, and 12–13 guests per capsule. Furthermore, their uptake is not accommodated by the expulsion of propionate ligands (a point confirmed using capsules with non-deuterated propionate ligands).

Of the hydrocarbons investigated, *n*-butane (C_4) appears to provide the best compromise between hydrophobic effects, which increase with alkane size, and steric crowding, which makes the entropic contribution to aggregation inside the capsule less favorable.[17c] Each capsule with 13 *n*-butane guests contains 52 related methyl and methylene groups, close to the sum of 58 methyl and methylene groups of the 29 propionate ligands. Moreover, each *n*-butane molecule has

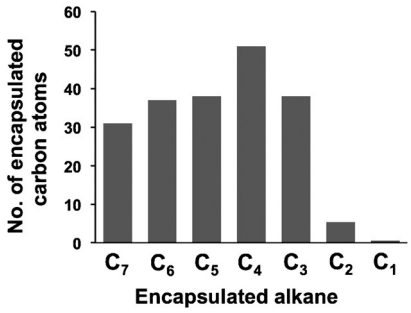

Figure 5. Numbers of carbon atoms for the C_7 to C_1 alkanes inside the [D_5]-propionate form of the {Mo_{132}}-type capsule, based on integration of the ^{1}H NMR signals in Figure 4.

a van der Waals (vdw) volume[19a] of 79 Å^3, such that 13 of these guests occupy a total volume of 1027 Å^3, which is much too large for the *n*-butane molecules to reside exclusively within the capsule's approximately 700 Å^3 central cavity (diameter: 11 Å; see Figure 3a). They can be accommodated, however, if they intercalate between the propionate ligands to form a hydrophobically assembled spherical shell, perhaps with the "tails" of the *n*-butane guests extending into the cavity at the center of the capsule. This was confirmed by using rotating-frame nuclear Overhauser effect NMR spectroscopy (ROESY)[18b] to locate the *n*-butane guests relative to the C_α and C_β hydrogen atoms of non-deuterated propionate ligands ($H_3C_\beta H_2C_\alpha CO_2^-$; Figure 6).

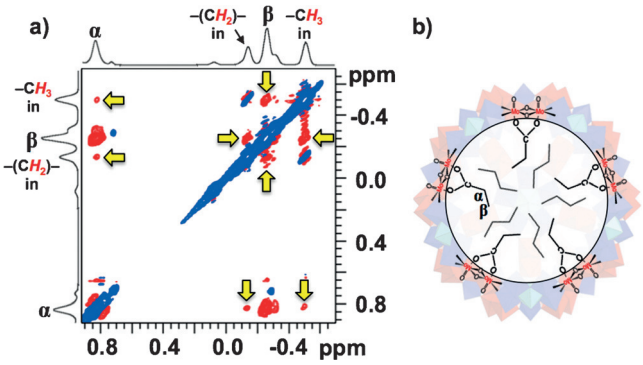

Figure 6. Location of *n*-butane guests inside the propionate ligand ($H_3C_\beta H_2C_\alpha CO_2^-$) form of the capsule. a) ROESY NMR spectrum with intra- and intermolecular interactions leading to negative ROE cross peaks (in red) and positive diagonal peaks (in blue). Yellow arrows indicate signals that are due to interactions between the -CH_2 and -CH_3 groups of *n*-butane with the C_α and C_β hydrogen atoms of the $H_3C_\beta H_2C_\alpha CO_2^-$ ligands. b) Two-dimensional cut-away diagram of the capsule showing five *n*-butane molecules intercalated between propionate ligands.

In the spectrum in Figure 6a, negative ROE cross peaks (yellow arrows) indicate strong interactions between protons from both the C_α and C_β atoms (at 0.8 and −0.25 ppm, respectively) and both the methylene (-CH_2-) and methyl (-CH_3) protons of *n*-butane ("in"). Notably, the -CH_2- groups lie within 2–3 Å[18b] of the protons attached to the C_α atoms of the propionate ligands. This specific interaction definitively locates numerous *n*-butane molecules between the propionate ligands, and under the capsule's twelve pentagonal {$Mo^{VI}_6O_{21}(H_2O)_6$} units, where sufficient space is available for accommodating the approximately 13 *n*-butane guests. This is illustrated by the two-dimensional cut-away view of the capsule in Figure 6b.

For ethane (C_2) and methane (C_1), the number of encapsulated carbon atoms was smaller by one order of magnitude (Figure 5). Notably, this is not due to the change from liquid hydrocarbons (including liquefied *n*-butane) to gases (C_3, C_2, and C_1): For all three of the latter compounds, D_2O solutions of the capsule were identically exposed to each gas at a pressure of 3 atm at 296 K. Nevertheless, a clear discontinuity was observed between propane (C_3) and the smaller alkanes.

For methane, half of the capsules contain a single molecule of CH_4, giving a ratio of encapsulated to externally dissolved CH_4 of 0.7. At the same time, the broad signal for CH_4 in bulk D_2O outside the capsule (at 0.1 ppm in Figure 4G) indicates rapid exchange—relative to the ^{1}H NMR timescale—with molecules of CH_4 inside the capsule. Given this dynamic exchange and the relatively small concentration of encapsulated CH_4, further investigation of the smaller alkanes focused on the behavior and location of ethane inside the capsule. Notably, with six chemically equivalent protons and an average value of 2.7 guests per capsule, the intensities of the ^{1}H NMR signals of encapsulated C_2H_6 were nearly one order of magnitude larger than those of CH_4 and much more amenable to analysis by ROESY NMR spectroscopy.[20]

Moreover, ^{1}H NMR spectra of encapsulated ethane revealed a phenomenon not seen in previous investigations of {Mo_{132}}-type or other water-soluble capsules. Two hours after the uptake of two or three molecules of ethane in each capsule (2.7 equiv overall), a distinct set of sharp signals was observed at −0.53 ppm (Figure 7).

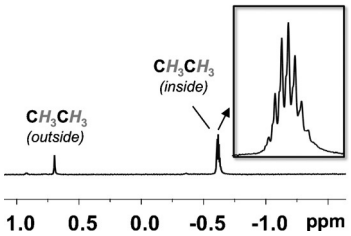

Figure 7. a) ^{1}H NMR spectrum of the capsule with encapsulated ethane (3 atm) after 2 h at 296 K. The ratio of encapsulated to externally dissolved molecules of ethane was 5.4.

The linewidths of the signals within the envelope of signals are similar to those of ethane dissolved in organic solvents, and dramatically narrower than the broad ^{1}H NMR signals observed until now for organic guests—including the C_7 to C_3 alkanes reported here—within {Mo_{132}}-type capsules. The distance (in Hz) between the individual signals increased from 2.5 to 3.2 to 4.5 Hz for spectra acquired on 400, 500, and 700 MHz instruments, respectively (Figure S5). These results show that the multiple signals are not due to *J* coupling between protons.[21] Instead, the multiple signals indicate that the encapsulated ethane molecules experience a range of slightly different chemical environments.[22] Aside from the seven sharp signals seen in Figure 7, other spectra in repeat experiments were found to feature up to ten sharp signals (observed using a 500 MHz instrument; Figure S5). To give rise to such narrow signals, the encapsulated ethane molecules must be rotating rapidly relative to the ^{1}H NMR timescale.

This situation, involving a narrow distribution of very similar chemical environments combined with rapid rotation, suggested that the ethane guests reside within the relatively isotropic 700 Å^3 hydrophobic cavity at the center of the capsule. This cavity is large enough to accommodate several ethane molecules,[19b] each with a van der Waals volume of 45 Å^3.[19a] The cavity is also largely, if not entirely, depleted of water (even before the reaction with ethane),[15e] further enabling the ethane molecules to rotate rapidly. Moreover, the discontinuity between the numbers of propane and ethane guests (12.7 vs. 2.7; Figure 5) is certainly consistent with an alkane-size-determined population of different domains within the capsule. Information concerning the location of encapsulated ethane was obtained by ROESY NMR spectroscopy, which indeed showed the ethane guests to reside within the central cavity of the capsule (Figure 8).

If an ethane molecule was located in the central cavity (Figure 8b), its dominant interactions should be with the

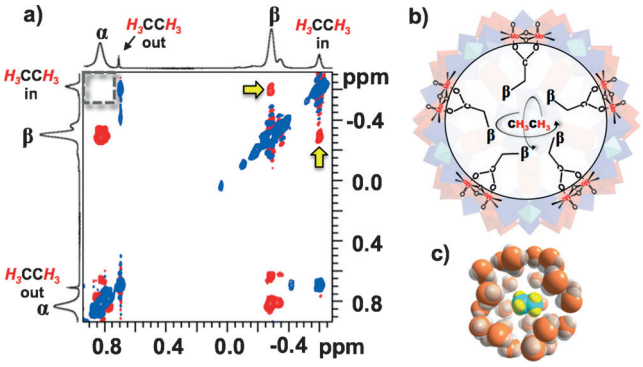

Figure 8. Location of ethane guests inside the propionate ligand ($H_3C_\beta H_2C_\alpha CO_2^-$) form of the capsule. a) ROESY NMR spectrum with yellow arrows indicating signals that are due to interactions between the ethane guests and the C_β hydrogen atoms of the $H_3C_\beta H_2C_\alpha CO_2^-$ ligands. Other signals are as described in the caption of Figure 6. b) Two-dimensional cut-away diagram showing the corresponding location and rotational motion of an ethane molecule present in the 11 Å diameter central cavity formed by the -$C_\beta H_3$ end groups of the propionate ligands. c) Space-filling model showing a 45 Å^3 ethane guest in the 700 Å^3 large central cavity (the color scheme is given in the caption of Figure 1).

protons of the β-carbon end groups (-$C_\beta H_3$) of the 29 $H_3C_\beta H_2C_\alpha CO_2^-$ ligands. In the ROESY NMR spectrum, prominent negative ROE cross peaks (in red) indicate strong interactions with those β-carbon protons; these are indicated by yellow arrows in the top-right corner of Figure 8a. In contrast to the ROESY spectrum of the capsule with *n*-butane guests, interactions between the ethane molecules and the α-carbon protons of the propionate ligands were not readily discernable.[24] This is seen by comparing the empty box in the top-left corner of the spectrum with the analogous region in the spectrum in Figure 6a. These data demonstrate a marked preference for ethane guests to reside within the 700 Å^3 central cavity defined by the -$C_\beta H_3$ end groups of the propionate ligands (Figure 6c).

Two ethane molecules (for example) occupy less than 1/8 of the cavity volume, leaving sufficient room to rotate rapidly on the ^{1}H NMR timescale, which results in the sharp signals in Figure 7. Interestingly, this bears some resemblance to alkane clathrates, where encapsulated hydrocarbons rotate rapidly in similarly sized cavities (8–11 Å diameter) formed by hydrogen-bonded water molecules.[25] Finally, viewed from an entirely different perspective, the effective "pressure" of ethane molecules in the largely empty cavities reported here

is similar to that in commercial gas cylinders: 115 bar for two ethane guests, and 173 bar for three molecules of ethane.[26]

In summary, the multiple lines of evidence provided above reveal that distinct host domains inside the propionate ligand form of the $\{Mo_{132}\}$-type nanocapsule are preferentially populated as a function of alkane size, giving strikingly different types of hydrophobic assemblies. Upon their uptake from water, 12 to 13 *n*-butane guests assemble between the propionate ligands, in space available under the twelve pentagonal $\{Mo^{VI}_6O_{21}(H_2O)_6\}$ units of the capsule. The ethyl tails of the propionate ligands, together with the *n*-butane guests, thus form a spherical supramolecular shell of up to 110 methyl and methylene groups. Owing to this tightly packed assembly, the motion of *n*-butane guests is restricted, as indicated by broad signals in the ^{1}H NMR spectra. A distinctly different hydrophobic domain is defined by the methyl end groups of the propionate ligands, which form a hydrophobic cavity at the center of the capsule. In this relatively large cavity, two or three ethane guests rotate rapidly relative to the ^{1}H NMR timescale, giving correspondingly sharp signals, a phenomenon never before observed for the uptake of alkanes from water by molecular cages or containers.

Acknowledgements

I.A.W. thanks the Israel Science Foundation (190/13), A.M. thanks the Deutsche Forschungsgemeinschaft (DFG) and generally speaking the ERC for an Advanced Grant, and the authors thank Dr. Alice Merca for high-quality graphics.

Keywords: alkanes · confinement effect · hydrophobicity · molybdenum · porous capsules

How to cite: *Angew. Chem. Int. Ed.* **2016**, *55*, 4476–4481
Angew. Chem. **2016**, *128*, 4552–4557

[1] a) J. Carroll, *Natural Gas Hydrates: A Guide for Engineers*, 2nd. ed., Elsevier, Burlington, MA, **2009**; b) E. D. Sloan, Jr., C. A. Koh, *Clathrate Hydrates of Natural Gases*, 3rd. ed., CRC Press, NW, **2007**; c) *Natural Gas Hydrates in Oceanic and Permafrost Environments* (Ed.: M. D. Max), Springer, Berlin, **2003**.

[2] a) W. Wang, A. D. Liang, S. J. Lippard, *Acc. Chem. Res.* **2015**, *48*, 2632–2639; b) S. Sirajuddin, A. C. Rosenzweig, *Biochemistry* **2015**, *54*, 2283–2294.

[3] J. Park, H. V. Pham, K. Mogensen, T. I. Solling, M. Vad Bennetzen, K. N. Houk, *J. Org. Chem.* **2015**, *80*, 997–1005.

[4] D. Ajami, J. Rebek, *Acc. Chem. Res.* **2013**, *46*, 990–999.

[5] a) Z. Takacs, E. Steiner, J. Kowalewski, T. Brotin, *J. Phys. Chem. B* **2014**, *118*, 2134–2146; b) V. Guralnik, L. Avram, Y. Cohen, *Org. Lett.* **2014**, *16*, 5592–5595; c) L. Avram, Y. Cohen, J. Rebek, Jr., *Chem. Commun.* **2011**, *47*, 5368–5375; d) L. Avram, Y. Cohen, *Org. Lett.* **2006**, *8*, 219–222; e) L. Garel, J.-P. Dutasta, A. Collet, *Angew. Chem. Int. Ed. Engl.* **1993**, *32*, 1169–1171; *Angew. Chem.* **1993**, *105*, 1249–1251; f) C. Browne, W. J. Ramsay, T. K. Ronson, J. Medley-Hallam, J. R. Nitschke, *Angew. Chem. Int. Ed.* **2015**, *54*, 11122–11127; *Angew. Chem.* **2015**, *127*, 11274–11279.

[6] F. Hof, J. Rebek, *Proc. Natl. Acad. Sci. USA* **2002**, *99*, 4775–4777.

[7] A. Scarso, L. Trembleau, J. Rebek, *J. Am. Chem. Soc.* **2004**, *126*, 13512–13518.

[8] Z. Laughrey, B. C. Gibb, *Chem. Soc. Rev.* **2011**, *40*, 363–386.

[9] S. Liu, D. H. Russell, N. F. Zinnel, B. C. Gibb, *J. Am. Chem. Soc.* **2013**, *135*, 4314–4324.

[10] H. Gan, C. J. Benjamin, B. C. Gibb, *J. Am. Chem. Soc.* **2011**, *133*, 4770–4773.

[11] a) S. Chen, M. Yamasaki, S. Polen, J. Gallucci, C. M. Hadad, J. D. Badjić, *J. Am. Chem. Soc.* **2015**, *137*, 12276–12281; b) Y. Ruan, P. W. Peterson, C. M. Hadad, J. D. Badjic, *Chem. Commun.* **2014**, *50*, 9086–9089; c) J. L. Bolliger, T. K. Ronson, M. Ogawa, J. R. Nitschke, *J. Am. Chem. Soc.* **2014**, *136*, 14545–14553.

[12] a) D. B. Smithrud, T. B. Wyman, F. Diederich, *J. Am. Chem. Soc.* **1991**, *113*, 5420–5426; b) D. B. Smithrud, F. Diederich, *J. Am. Chem. Soc.* **1990**, *112*, 339–343.

[13] a) W. M. Nau, M. Florea, K. I. Assaf, *Isr. J. Chem.* **2011**, *51*, 559–577; b) M. Florea, W. M. Nau, *Angew. Chem. Int. Ed.* **2011**, *50*, 9338–9342; *Angew. Chem.* **2011**, *123*, 9510–9514; c) Y. Miyahara, K. Abe, T. Inazu, *Angew. Chem. Int. Ed.* **2002**, *41*, 3020–3023; *Angew. Chem.* **2002**, *114*, 3146–3149.

[14] Y. H. Ko, H. Kim, Y. Kim, K. Kim, *Angew. Chem. Int. Ed.* **2008**, *47*, 4106–4109; *Angew. Chem.* **2008**, *120*, 4174–4177.

[15] Hydrophobic interactions are of general importance and play a key role in numerous biological and industrial processes; see: a) C. Tanford, *The Hydrophobic Effect: Formation of Micelles and Biological Membranes*, 2nd ed., Wiley, New York, **1980**; b) P. C. Nelson, M. Radosavljević, S. Bromberg, *Biological Physics: Energy, Information, Life*, W. H. Freeman, New York, **2008**; c) H.-J. Schneider, *Acc. Chem. Res.* **2015**, *48*, 1815–1822; d) F. Biedermann, W. M. Nau, H.-J. Schneider, *Angew. Chem. Int. Ed.* **2014**, *53*, 11158–11171; *Angew. Chem.* **2014**, *126*, 11338–11352; e) A. Müller, S. Garai, C. Schäffer, A. Merca, H. Bögge, A. J. M. Al-Karawi, T. K. Prasad, *Chem. Eur. J.* **2014**, *20*, 6659–6664; f) W. Blokzijl, J. B. F. N. Engberts, *Angew. Chem. Int. Ed. Engl.* **1993**, *32*, 1545–1579; *Angew. Chem.* **1993**, *105*, 1610–1650.

[16] a) S. Kopilevich, A. Müller, I. A. Weinstock, *J. Am. Chem. Soc.* **2015**, *137*, 12740–12743; b) S. Kopilevich, A. Gil, M. Garcia-Ratés, J. Bonet-Ávalos, C. Bo, A. Müller, I. A. Weinstock, *J. Am. Chem. Soc.* **2012**, *134*, 13082–13088; c) A. Ziv, A. Grego, S. Kopilevich, L. Zeiri, P. Miro, C. Bo, A. Müller, I. A. Weinstock, *J. Am. Chem. Soc.* **2009**, *131*, 6380–6382; d) N. Watfa, D. Melgar, M. Haouas, F. Taulelle, A. Hijazi, D. Naoufal, J. B. Avalos, S. Floquet, C. Bo, E. Cadot, *J. Am. Chem. Soc.* **2015**, *137*, 5845–5851.

[17] For a Concept Article on Mo_{132}, see: a) A. Müller, P. Gouzerh, *Chem. Eur. J.* **2014**, *20*, 4862–4873; see also: b) A. Müller, P. Gouzerh, *Chem. Soc. Rev.* **2012**, *41*, 7431–7463; c) A. Grego, A. Müller, I. A. Weinstock, *Angew. Chem. Int. Ed.* **2013**, *52*, 8358–8362; *Angew. Chem.* **2013**, *125*, 8516–8520; d) C. Schäffer, A. M. Todea, H. Bögge, O. A. Petina, D. Rehder, E. T. K. Haupt, A. Müller, *Chem. Eur. J.* **2011**, *17*, 9634–9639; e) C. Schäffer, H. Bögge, A. Merca, I. A. Weinstock, D. Rehder, E. T. K. Haupt, A. Müller, *Angew. Chem. Int. Ed.* **2009**, *48*, 8051–8056; *Angew. Chem.* **2009**, *121*, 8195–8200.

[18] a) C. S. Johnson, Jr., *Prog. Nucl. Magn. Reson. Spectrosc.* **1999**, *34*, 203–256; b) H. Friebolin, *Basic One- and Two-Dimensional NMR Spectroscopy*, 5th ed., Wiley-VCH, Weinheim, **2010**.

[19] a) A. Bondi, *J. Phys. Chem.* **1964**, *68*, 441–451; b) according to the 55 % rule (see Ref. [19c]), the 700 Å^3 central cavity should be capable of hosting up to 8 or 9 equiv of ethane. Based on the effect of ethane pressure on uptake (see the Supporting Information), this value, corresponding to optimal binding, might indeed be reached if the ethane pressure was increased to 9 atm; c) S. Mecozzi, J. Rebek, Jr., *Chem. Eur. J.* **1998**, *4*, 1016–1022.

[20] Considering six chemically equivalent protons for C_2H_6, versus four for CH_4, and the larger average number of equivalents of

encapsulated ethane (i.e., 2.7 vs. 0.5 for CH_4), the ^{1}H NMR signals of the ethane guests were eight times more intense than those of methane.

[21] The groups of Cohen and Rebek observed similar phenomena for occluded molecules of halocarbon solvents in hydrogen-bonded (organic-solvent-soluble) pyrogallol[4]arene capsules; see Refs. [5b–d]. Following their lead, we used changes in the NMR field strength and DOSY NMR spectroscopy (Figure S4) to conclude that the set of sharp signals is due to rapidly rotating guest molecules in slightly different encapsulation environments.

[22] This is not surprising as each capsule is populated by either two or three ethane molecules (an average of 2.7 equiv was determined by ^{1}H NMR spectroscopy). Furthermore, the number of propionate ligands in each capsule may vary slightly, from 28 to 30 (i.e., 29 ± 1), and these may undergo exchange between the 30 $\{Mo^{V}_2O_4L\}$ binding sites and less well defined sites under the 12 pentagonal $\{Mo^{VI}_6O_{21}(H_2O)_6\}$ units (see Ref. [23]). These slightly differing chemical environments give rise to a Gaussian distribution of closely separated signals.

[23] O. Petina, D. Rehder, E. T. K. Haupt, A. Grego, I. A. Weinstock, A. Merca, H. Bögge, J. Szakacs, A. Müller, *Angew. Chem. Int. Ed.* **2011**, *50*, 410 – 414; *Angew. Chem.* **2011**, *123*, 430 – 434.

[24] By greatly increasing the intensity used in plotting, the resultant spectrum, albeit very "noisy", includes a small cross peak indicative of a weak interaction between ethane and the α-carbon protons of the propionate ligands. This is attributed to the 109° O_2C-C_α-C_β angle of the ligand in combination with bending about the C_α atom and dynamic room-temperature "tilting" of the entire η^2-bound ligand relative to the dimolybdenum linkages of the capsule.

[25] a) E. D. Sloan, *Nature* **2003**, *426*, 353 – 363; b) D. W. Davidson, C. I. Ratcliffe, J. A. Ripmeester, *J. Incl. Phen.* **1984**, *2*, 239 – 247.

[26] For two ethane guests, $P = nRT/V$, with $n = 2 \times (6.022 \times 10^{23}\ \text{mol}^{-1})^{-1}$, $R = 82.06\ \text{cm}^3\,\text{atm}\,\text{mol}^{-1}\,\text{K}^{-1}$, $T = 296$ K, and $V = 7 \times 10^{-22}\ \text{cm}^3$.

Received: December 7, 2015
Revised: January 12, 2016
Published online: February 15, 2016

